Tellus (1994), 46A, 113–133
Printed in Belgium – all rights reserved

TELLUS
ISSN 0280–6495

Numerical modeling of the Halten Bank area: a validation study

By BRUCE HACKETT and LARS PETTER RØED*, *Nansen Environmental and Remote Sensing Center, Vollsveien 13, Bygg B, N-1324 Lysaker, Norway*

(Manuscript received 2 December 1992; in final form 6 August 1993)

ABSTRACT

From observations and simple model simulations, it has been established that a proper model of the Halten Bank area must, as a minimum, (i) include the *barotropic* component and at least one *baroclinic component*, (ii) allow *shear instabilities* to properly grow into eddies, (iii) include *vertical mixing* to allow for entrainment of lower layer water masses into the upper layer, (iv) allow for *advection* of density (temperature and salinity) in the upper water masses, and (v) allow the inclusion of tides. All of these physics factors are included in the mathematical formulation of fully three-dimensional numerical ocean models. Two such models, arbitrarily named the POM model and the SINMOD model, have been used to simulate the current, salinity and temperature structure in the Halten Bank area for March 1988 and then validated against the Norwegian Continental Shelf Experiment 1988 (NORCSEX'88) data set. Although the motion in the two models is governed by the same set of continuous equations, an inspection of the parameterizations and numerical methods employed to solve the governing equations reveals that the SINMOD model should be expected to provide smoother and less energetic results than the POM model. It is also speculated that eddy growth is inhibited in both models due to (i) the tendency of level models to create fictitious diapycnal mixing in areas of sloping density surfaces, and (ii) too coarse resolution. These conclusions are partially supported by the validation analysis. In order to facilitate a meaningful model-model comparison and validation, specific products were provided by careful analyses of both data and model results in accordance with a preselected hierarchic set of comparison criteria. The criteria focus on mean circulation patterns and horizontal and vertical distributions. The analyses reveal that the most probable limitation inhibiting the models in reproducing the observed structures is the lack of horizontal resolution. The chosen grid mesh size (4 km) only barely resolves the eddy scale dictated by the Rossby radius of deformation, thus inhibiting eddy growth due to shear instabilities. Further, both this and earlier studies conclude that it is an open question how complex a model needs to be to be able to simulate the observed structure to a satisfactory degree.

1. Introduction

The Halten Bank is located on the continental shelf off mid-Norway (see Fig. 1). With its traditionally rich fisheries and expanding oil activity, the oceanography of the Halten Bank and surrounding waters has been given considerable attention over the past decade. Recently, efforts have been made to utilize numerical ocean models to determine the circulation of the shelf region and, hopefully, to improve design currents for offshore activities. A major initiative was put forth by the Norwegian oil industry, which has funded a research program aimed at implementing an operational three-dimensional model for the region. The program consists of phases: In the first phase, a small number of candidate models were selected from a proposed group of existing models. Here, the term "model" is used in narrow sense, meaning the computer code running at a particular institution. The first phase resulted in the selection of two models, which participated in a

* Corresponding author.

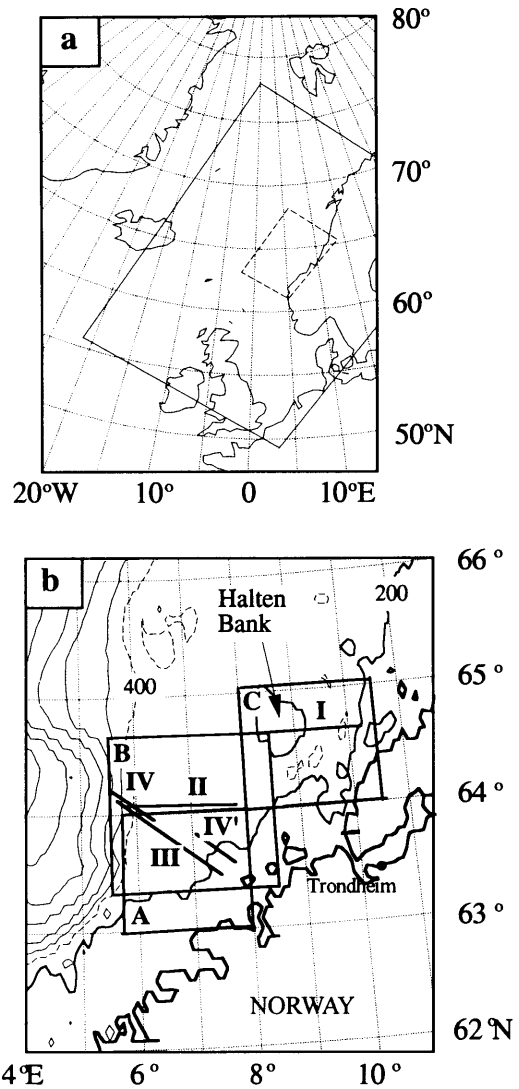

Fig. 1. Map of the Nordic Seas and the Halten Bank area. The coarse grid model domain corresponds to the solid skewed rectangle inside of (a), while the fine mesh model domain corresponds to the dashed rectangle embedded within the coarse mesh. In (b) is shown a close up of the Halten Bank area. Also shown is the horizontal mapping areas (heavy boxes) denoted A, B, and C and the vertical sections denoted I, II, III, IV, and IV′ (semi-heavy lines) for data collected during the NORCSEX'88 field experiment. The coastline is revealed by the heavy line, while the 200 m depth contour is shown in semi-heavy solid lines. The shelf break roughly follows the 400 m depth contour, which is shown as a dotted line. Otherwise the topography is shown by thin lines with a contour interval of 200 m.

second phase. In the second phase, the candidate models were implemented for the Halten Bank region and tested, against both observations and each other. The results of the second phase are the subject of this paper, while results from the first phase may be found in Røed et al. (1989).

Numerical modeling of the currents near the Halten Bank has been limited prior to the study which is discussed here. Several barotropic models have been applied with the aim of investigating storm surges (Martinsen et al., 1979) and tides (Gjevik and Straume, 1989). These models have demonstrated great skill at reproducing water levels and tidal currents, and show that the barotropic mode is a major component of the total current field on the shelf. However, they intrinsically lack the baroclinic modes and density variations, and offer poor (or no) information on the vertical current structure. In particular, barotropic models cannot generate the mesoscale eddies which are so ubiquitous on the shelf. Haugan et al. (1991) directly addressed the question of eddy-generation by applying a two-layer quasi-geostrophic model to the region. This simple model, which used an idealized geometry and topography, was able to reproduce many features of the observed mesoscale variability, thereby demonstrating the strong influence of topography and baroclinic instability on the currents. However, the quasigeostrophic assumption implicitly filters out inertia-gravity waves (e.g., Kelvin waves), which are not insignificant components of the total current field in the area.

The successes and deficiencies of these earlier modeling efforts with regard to the three-dimensional current field indicate the requirements for more sophisticated and, presumably, more accurate models. It was against this background that the oil industry landed on the concept of a fully three-dimensional, primitive equation baroclinic model for currents in the Halten Bank region. It was felt that only such a model could include the important physical processes on the shelf, on the temporal and spatial scales required. There are basically two choices for such a model, namely a layered model or a level model. In the previous phase of this study, a layered model, similar to the model applied by Thompson and Schmitz (1989) to reproduce the Gulf Stream eddies, was shown by Røed et al. (1989) to be equally suitable for the task at hand compared to

the level models. Unfortunately, this model was not available for the present study. Still, within the class of level models, there are a number of approaches, based on different physical formulations, subgrid-scale parameterizations, numerical schemes, etc. As pointed out by Chassignet (1992), in order to select such a suitable model, it is necessary to make a careful examination and comparison of each model's physical fundaments, interpretability, and numerical efficiency, not to mention applicability to the particular application at hand.

The primary focus of the model-observation comparison described in the following is on currents, and an effort is made to assess how well the models agree with observations during a given simulation period. There is no standard procedure for making such a comparison, and the criteria for agreement formulated by two investigators will no doubt differ. In the present work, a hierarchy of comparison products is used, starting with the most overall, or "integral," types and working down to more spatially and temporally detailed products. The rationale for this classification is that, only if the models reproduce the most general features (is the main flow northward?) is it worthwhile to look at more detailed comparisons (say, grid point currents against a current meter).

A brief review of the physical setting and the currents in the Halten Bank region is given (Section 2), the purpose of which is to elucidate the capabilities which a model should contain. Thereafter, Section 3 describes the two models and how they were implemented and run for the simulation period. Section 4 describes the set of field observations selected for the validation, the NORCSEX'88 data. The model-observation comparison is described and discussed in Section 5. The final Section (6) contains a summary and some concluding remarks.

2. The physics of the Halten Bank area

The mid-Norwegian continental shelf (Fig. 1a) is characterized by mean depths of some 300 m, with several shallower banks ($\sim$100 m) and deeper troughs ($\sim$450 m) complicating the bottom relief. It is bounded by the very irregular coastline on one side and a steep continental slope on the other. In the south, the shelf is narrow and shallower ($\sim$200 m). Going northward, it widens to a maximum of about 200 km, and deepens. Its northward extent may be delimited by the Lofoton archipelago, where the shelf again narrows dramatically. The Halten Bank is a major feature of the area, rising to $\sim$100 m depth and separated from the coast by a deep trough (400 500 m depth). In the following, most attention will be given to the southern part of the shelf, since the field observations used in the validation are concentrated there.

Two water masses determine the hydrography on the shelf: Atlantic water and coastal water. The Atlantic water mass, which enters the area from the Faroe-Shetland Channel (McCartney and Talley, 1984), is saline (>35 psu) and of fairly constant temperature (6°–8°) year-round. It is associated with the Norwegian Atlantic Current (NAC), which flows northward along the continental shelf slope. The coastal water mass, which is composed of water from the Baltic, the North Sea and freshwater run-off, is characterized by lower salinity and more strongly varying temperature; in winter and early spring, it is colder than the Atlantic water. It is associated with the Norwegian Coastal Current (NCC), which flows generally northward along the coast from the Skagerrak to the Barents Sea. It should be recalled that, in this range of salinities and temperatures, the density is determined largely by salinity. Furthermore, in these waters, the temperature field nearly parallels the salinity.

These two water masses meet in the southern part of the region, and a sharp surface front is formed between them. In a vertical cross-section, they form a characteristic coastal two-layer system. The coastal water appears as an upper layer wedge, with maximum depths of 50–100 m, lying above the lower layer Atlantic water. Between them is a relatively sharp pycnocline, which is essentially parallel to the halocline. The lateral extent of the coastal water varies greatly, but the NCC coastal jet has a width of $\sim$10 km, which, not surprisingly, accords with the typical internal Rossby radius of deformation (5–10 km). In the narrow southern part of the shelf, the front appears to follow the shelf break (Haugan et al., 1991). As the shelf widens and deepens northward, the topographic constraint on the front weakens and the front becomes more unstable. Topographic features on the shelf, like troughs and banks, can then induce the formation of intense

mesoscale structures. Infrared satellite imagery from the area show an abundance of eddies, meanders and streamers (Haugan et al., 1991). In addition, topographic variations along the shelf break tend to steer Atlantic water onto the shelf in preferred areas.

In the vicinity of the Halten Bank, the NCC jet narrows and accelerates under the influence of the offshore bank and the deep intervening trough. Around the bank itself, there is a tendency to anticyclonic circulation, probably due to Taylor column dynamics (Eide, 1979). This circulation is most likely in the winter when the stratification is weakest, and it can cause a counter-current (towards the SW) on the shoreward flank of the bank.

On average, the NCC transport is less than 0.5 Sv (1 Sv = 10^6 m^3 s^{-1}), varying from 0 to 1 Sv. Observed speeds vary from 0 to over 1 m s^{-1}, with a winter average of about 0.2 m s^{-1} (Eide, 1979). The corresponding transport magnitudes for the NAC are not well known, but they are certainly larger. McCartney and Talley (1984) proposed a value of about 5 Sv, based on heat and mass balances, and that figure is sufficient for the present use (the two participating models used this figure). Current measurements in the NAC at the shelf break show typical speeds of up to 1 m s^{-1}.

In terms of the physical processes which determine the current field on the shelf, the NAC and NCC have quite different origins. The NAC is a branch of the general thermohaline circulation of the North Atlantic, Nordic and Polar Seas, and may therefore be considered an external influx to Norwegian waters. The NCC, on the other hand, is largely a result of density differences which originate in the Nordic region (Gammelsrød and Hackett, 1981).

In addition to the two semi-permanent currents and the mesoscale eddy field, the current field has a strong atmospherically forced component on time scales of several days. This forcing is effected not only through local wind traction and pressure changes, but through up- and downwelling events whose signals propagate along the coast as internal Kelvin waves. It is largely this component which accounts for the extreme velocities and transports which have been observed. Furthermore, there are inertial oscillations connected with wind events which may cause current velocities of $\sim$0.1 m s^{-1} (Eide, 1979). Finally, tidal currents, which have amplitudes of 0.05–0.15 m s^{-1} and large spatial variations (Gjevik and Straume, 1989), make a modest but not insignificant contribution to the total current.

With reference to model capabilities, the important physical features of the current field in the Halten Bank region are: (a) density stratification, (b) externally determined boundary fluxes, (c) topographic effects, (d) mesoscale structures, (e) wind forcing, (f) tides. In order to be able to reproduce such features, a model must include the following.

(1) The barotropic mode, in order to include topographic effects and the tides.

(2) At least one baroclinic mode, so as to allow for both baroclinic and barotropic instability mechanisms.

(3) Vertical mixing, in order to allow for the entrainment of underlying Atlantic water into the coastal water.

(4) Advection of temperature and salinity (density) in the upper water masses, so as to allow the formation of dipole eddies and streamers along the front.

(5) In connection with 2 and 4, it is necessary that shear instabilities be allowed to properly grow into eddies, i.e., there should not be excessive damping.

(6) Diverse boundary conditions, so as to accommodate bottom topography, local wind forcing and externally driven currents in realistic simulations.

3. The two models employed

Model results from simulations with two fully three-dimensional numerical models belonging to the class of level models (as opposed to layered or isopycnal models) were made available for this validation study. Such models certainly include, if properly implemented, the necessary components presented at the end of the previous section. Attempts to include a layer model in this study for comparison with the level models unfortunately failed. The two models will henceforth arbitrarily be referred to as the POM model and the SINMOD model. A detailed description of the POM model, including the methods used to produce the model results presented below, may be

found in Oey and Chen (1992a, b). A less detailed description of the SINMOD model may be found in Slagstad and Støle-Hansen (1991). A complete set of the simulation results from the two models as used in the validation study and presented in a uniform fashion, may be found in Hackett and Røed (1992). The POM model is a version of the Princeton Ocean Model, the details about which may, in addition to Oey and Chen (1992a, b), be found in Blumberg and Mellor (1987). For further details on the SINMOD model the reader is referred to Slagstad (1987). Only a limited description of the two models will be provided here to help the reader appreciate the similarities and differences between them and the possible implications this may have on the model-model comparison and on the validation.

Both models are based on a standard formulation of the conservation equations for momentum and mass, utilizing the hydrostatic and the Boussinesq approximations, viz.

$$\rho_0(\boldsymbol{u}_t + \boldsymbol{u}\cdot\nabla\boldsymbol{u} + w\boldsymbol{u}_z + f\boldsymbol{k}\times\boldsymbol{u}) = -\nabla p + (A_v\boldsymbol{u}_z)_z + \boldsymbol{F}, \tag{3.1}$$

$$p_z = -\rho g, \tag{3.2}$$

$$e_t + \boldsymbol{u}\cdot\nabla e + we_z = (K_v e_z)_z + \nabla\cdot(K_H\nabla e), \tag{3.3}$$

$$\nabla\cdot\boldsymbol{u} + w_z = 0, \tag{3.4}$$

$$\rho = \rho(S, T). \tag{3.5}$$

Here, $\boldsymbol{u}$ is the horizontal velocity, with components (u, v), and w is the vertical velocity component. ∇ is the horizontal gradient operator, f is the Coriolis parameter, $\boldsymbol{k}$ is the vertical unit vector, ρ_0 is a reference density, p is pressure, A_v is the vertical eddy viscosity, g is the gravitational acceleration, z is the vertical coordinate (positive upwards), e represents either temperature T or salinity S, and K_v and K_H are the associated vertical and horizontal eddy diffusivities, respectively. The density ρ is related to salinity and temperature through an equation of state (3.5). Both models assume the water masses to be incompressible, leading to the simple conservation equation (3.4). $\boldsymbol{F}$ refers to the horizontal mixing term added to parameterize sub-grid scale processes, i.e., processes that are not resolved by the chosen grid size. Their role is further to damp out the grid scale noise in the model to prevent this noise from growing through nonlinear (numerical) instabilities. Subscripts z and t refer to a derivative with respect to the subscript.

The first major difference between the two models is in their parameterization of the horizontal mixing term $\boldsymbol{F}$ (Table 1). The SINMOD model uses the commonly applied eddy viscosity concept, i.e.,

$$\boldsymbol{F} = A_H\nabla^2\boldsymbol{u}, \tag{3.6}$$

where A_H is the (constant) horizontal eddy viscosity, while the POM model uses the somewhat more complicated parameterization credited to Smagorinsky (1963), i.e.,

$$\boldsymbol{F} = \nabla\cdot\mathfrak{R},$$

$$\mathfrak{R} = \begin{bmatrix} 2A_H u_x & A_H(u_y + v_x) \\ A_H(u_y + v_x) & 2A_H v_y \end{bmatrix}. \tag{3.7}$$

In SINMOD, A_H and K_H are (rather large) constants, while in POM these are given by the formula

$$A_H = K_H = C\,\Delta x\,\Delta y \times [u_x^2 + v_y^2 + \tfrac{1}{2}(u_y + v_x)^2]^{1/2}, \tag{3.8}$$

where Δx and Δy are the horizontal grid distances and C is a constant. In the applications shown here, the reported values for the eddy viscosity are

Table 1. *Major physical differences between the POM and the SINMOD model*

Variable or parameter	Symbol	POM	SINMOD
vertical coordinate	—	σ-coordinates	z-coordinates
vertical eddy viscosity and diffusivity	A_v, K_v	computed using Mellor and Yamada (1982) formulation	computed using Richardson number formulation
horizontal eddy viscosity and diffusivities	A_H, K_H	computed using Smagorinsky (1963) formulation	constant in time and space

in the range 2–12 $m^2 s^{-1}$ for the POM model, while the SINMOD model uses a constant value of 50 $m^2 s^{-1}$.

It should be noted that the use of too large values for A_H and K_H may result in excessive smoothing, which in turn inhibits proper growth of eddies due to barotropic and baroclinic instabilities (Stern, 1975). This is further compounded by the fact that level models in general tend to create fictitious cross-isopycnal (diapycnal) mixing in areas of sloping isopycnals (Huang and Bryan, 1987). This is unwanted from a physical point of view since mixing in the ocean is predominantly along isopycnals. The Smagorinsky parameterization, which according to (3.7) and (3.8) is limited to areas of large shear, tends to reduce this fictitious diapycnal mixing and hence constitutes a physical improvement over the parameterization utilized by the SINMOD model. It should be noted however, that POM, in addition to the Smagorinsky formulation, uses an explicit filter to damp the grid scale noise. This effectively enhances the horizontal mixing.

Another major difference between the two models is found in the treatment of the vertical coordinate. While the SINMOD model discretizes the equations in a Cartesian coordinate system, POM first transforms the governing equations to a terrain-following coordinate system (commonly referred to as σ-coordinates) before the continuous equations are discretized. In such a system the vertical coordinate is transformed according to the equation

$$\sigma = \frac{z - \eta}{H + \eta}, \tag{3.9}$$

where η is the deviation of the free surface from its equilibrium position ($z = 0$) and H is the equilibrium depth of a water column (Oey and Chen, 1992a, b).

The final major difference in the physical formulation of the two models is in the parameterization of the vertical eddy viscosity and diffusivity (Table 1). Many of the processes that influence the magnitude of the diffusion coefficient for salinity, temperature and momentum (eddy viscosity) are poorly known. However, these processes significantly influence the dispersion and diffusion (mostly diapycnal mixing) of these quantities, as well as the associated flow field. In the SINMOD model, the eddy viscosity and the vertical diffusion are functionally dependent on the Richardson number. In the POM model, a higher order turbulence closure scheme credited to Mellor and Yamada (1982) is applied to compute these coefficients. In the latter formulation, the turbulent energy is allowed to be advected, i.e., areas containing events of large vertical mixing may export these events by advection. Again, the choice made in the POM model is more complex and sophisticated than in the SINMOD model.

In short, the parameterizations of the horizontal and vertical mixing terms are more complex in the POM model. In this connection it is interesting to note that the use of increasingly more sophisticated formulations of these processes, particularly formulations based on poorly known physics with an associated high degree of uncertainty, does not in itself necessarily reduce the uncertainty in the final model results (GESAMP, 1991). Although the parameterizations utilized in the POM model are more complex and sophisticated than those in the SINMOD model, they are nevertheless based on an improved understanding of the underlying physical processes. Thus, the POM model is, at least theoretically, expected to produce results that have less uncertainty.

The two models also differ in the numerical methods employed in the integration of the governing equations (Table 2). In the POM model,

Table 2. *Numerical characteristics of the two models POM and SINMOD*

Equation	Name	POM	SINMOD
momentum	time differencing	leap frog + mode splitting	semi-implicit + mode splitting
(eq. 3.1)	space differencing	centered	centered + upstream in space
mass	time differencing	leap frog + mode splitting	semi-implicit + mode splitting
(eq. 3.3)	space differencing	centered	upstream
	open boundaries	nesting + FRS	nesting + FRS

FRS = Flow Relaxation Scheme (Martinsen and Engedahl, 1987).

special care has been exercised to prevent artificial numerical fluxes, diffusion, dispersion and dissipation when choosing the numerical methods. Most of the code is explicit, eliminating the dissipation inherent in implicit or semi-implicit schemes. Further, care has been taken to employ schemes which conserve integral quantities, such as potential vorticity, kinetic energy, etc. The POM code is also computationally more efficient in that efforts have been made to optimize the code. These latter points are the result of the model having been extensively used and improved upon by several scientists over the years. In short, POM is a mature model that has been subject to many of the stages of a "quality assurance procedure" as defined by GESAMP (1991), i.e., to aspects related to model verification, sensitivity tests and validation. This is not the case for SINMOD. It is a rather "young" model, and may be said to be in its infancy regarding procedures relating to quality assurance.

The model results were produced by the following procedure (for details the reader is referred to Oey and Chen, 1992a). A fine mesh grid (4 km mesh size) covering the area 61°–66° N latitudes and 2° W–12° E longitudes was embedded within a coarse mesh model grid (20 km mesh size) defined approximately by the 51°–76° N latitudes and 20° W–22° E longitudes (Fig. 1a). A dynamic coupling between the 2 grids was allowed for (Oey and Chen, 1992a), in which the solution within the fine mesh area was driven by the values derived from the coarse mesh solution around the boundaries of the fine mesh area.

The simulation was initialized from a 585 days' quasi-equilibrium calculation, and included realistic meteorological forcings, inflows/outflows across the open boundaries (inflow of the North Atlantic warm water in particular), tides, coastal and Baltic discharges, and wintertime hydrography for model depths larger than about 500 m. This 585 day spin-up consisted of 3 stages. The first stage (days 0–150) was a diagnostic preprocessing run in which the model was forced by the Levitus (1982) climatology and the Hellerman and Rosenstein (1983) wind stress to find the boundary elevations associated with the mean climatological wind forcing and the large scale inflow of North Atlantic water. The second stage (days 150–345) was initialized from the previous stage and consisted of a semi-prognostic run with tides only (assuming that the mean climatological wind is inherent in the specified boundary elevation from the previous diagnostic run). In the third stage (days 345–585), again initialized from the previous stage, the realistic wind and discharge forcings for February and March 1988 (60 days), as detailed by Engedahl and Martinsen (1988), were applied cyclically four times.

The model products used in the present validation exercise were derived from a fifth cycle (60 days) starting at the end of the 585 day spin-up. Again the observed wind and discharge forcing for February and March 1988 were used. Various model products were then archived for later validation against archived observational products, as explained in Section 5.

4. The NORCSEX'88 data set

The NORwegian Continental Shelf EXperiment (NORCSEX) was carried out in March 1988 in the vicinity of the Halten Bank on the Norwegian shelf. The primary aim of the experiment was to collect validation data for the ERS-1 satellite. The field program included observations of hydrography and currents both from moored current meters and from a moving ship. In addition, many measurements with direct relevance to remote sensing were performed. Scientific results from the experiment are published in a special section in Journal of Geophysical Research (Johannessen, 1991). The NORCSEX'88 data

Table 3. *Horizontal areas from NORCSEX'88 selected for use in the evaluation study (cf. Fig. 1b)*

Name	Time span	Latitude	Longitude
A	25 March 1988 18:00–26 March 1988 16:00	63°00′–64°00′N	5°45′– 8°00′E
B	16 March 1988 08:00–19 March 1988 19:00	63°20′–64°40′N	5°30′– 8°30′E
C	13 March 1988 07:00–16 March 1988 08:00	64°00′–65°05′N	8°00′–10°30′E

Table 4. *Vertical sections from NORCSEX'88 selected for use in the validation study (cf. Fig. 1b)*

Name	Time span	Start position	End position	Ship's heading
I	13 March 1988 2110–2400	64°40′N 8°00′E	64°40′N 10°15′E	90°
II	16 March 1988 0815–1300	64°06′N 7°50′E	64°09′N 5°50′E	273°
III	20 March 1988 0920–1800	63°27′N 7°28′E	64°12′N 5°44′E	315°
IV	21 March 1988 0450–0830	64°15′N 5°35′E	63°57′N 6°18′E	315°
IV′	25 March 1988 1750–2100	63°50′N 7°05′E	63°36′N 7°45′E	315°

has later been analyzed with a model validation purpose in mind (Johannessen and Haugan, 1991, henceforth JH). The resulting data products, along with the relevant literature, constitute the observational input to the present work.

The ship-borne observations are perhaps the most interesting from the viewpoint of model validation. Since the ship was moving, it is possible to obtain a quasi-synoptic picture of the horizontal fields. The hydrographic measurements, i.e., temperature and salinity, were performed with a CTD sonde mounted in a towed undulator. This vehicle was configured to undulate over a nominal depth range 0–130 m. The current measurements were made with an ADCP, which obtained vertical current profiles between 10 m below the surface and 10–20 m above the bottom with 4 m resolution. With a typical ship speed of 7.5 knots, the horizontal resolutions were 1000 m for the temperature and salinity profiles and 600 m for the current profiles.

On the basis of the observations, three horizontal mapping areas and five vertical sections were selected, together with the current meter mooring sites, for comparison with model results. The 3 areas and 5 vertical sections are defined in Tables 3, 4, and displayed in Fig. 1b.

5. Model-observation comparison

In order to perform a meaningful model-model comparison and a model validation a set of assessment criteria has to be chosen. The philosophy behind the criteria chosen for this study is to order them in a hierarchy, in which the priority is assigned according to the level of spatial specificity in the products to be compared, with the highest priority to the most "integral" products. The 5 criteria with highest priority are: (i) the mean circulation, (ii) the sea level variability, (iii) volume transport through vertical sections, (iv) the horizontal distributions, and (v) the vertical distributions.

These criteria were originally formulated on the basis of the available observational products shown in JH, and on the assumption (hope) that the corresponding model products were available or could readily be produced. This assumption, unfortunately, did not prove to hold. In particular, model output specifically designed for testing criteria (i) and (ii) was not available. Both modeling groups did, however, make available horizontal sections, vertical sections and point time series corresponding to the ship and mooring data collected during NORCSEX'88. Thus, it is still possible to address the basic issue involved in criterion (i)—the general circulation pattern—using the three horizontal mappings (cf. Fig. 1b). On the other hand, suitable time series of the surface elevation field are not available from the models, so that a test according to criterion (ii) must be neglected.

Thus, the model-observation comparison starts with a comparison of volume transports, and continues with a comparison of the horizontal and vertical distributions. The question about the general pattern of the mean circulation is addressed in the section on horizontal distributions. Although the main topic of this study is currents, some attention will be given to the salinity and temperature, as they offer valuable insight into the workings of the models. In the following, results from the models will, as a rule, be presented in alphabetical order, i.e., POM, then SINMOD.

5.1. Volume transport through vertical sections

The volume transport was calculated for each of the vertical sections defined in Table 4 and shown

Table 5. *Volume transport in Sv (10^6 m^3 s^{-1}) through vertical sections, 0–250 m (cf. Fig. 1b and Table 4)*

Section	Observed (ADCP) N	S	Total	POM N	S	Total	SINMOD N	S	Total
I	+0.858	−0.477	+0.381	+1.141	−0.217	+0.923	+0.580	−0.391	+0.190
II	+0.378	−0.967	−0.589	+0.620	−0.410	+0.210	+0.600	−0.164	+0.436
III	+2.148	−1.396	+0.752	+2.857	−0.302	+2.555	+2.272	−0.109	+2.163
IV	+1.495	−0.006	+1.489	+0.907	−0.000	+0.907	+0.993	−0.000	+0.993
IV′	+0.649	−0.686	−0.037	+0.319	−0.100	+0.219	+0.494	−0.140	+0.354

Positive values indicates northward transport. The columns N and S indicate how much of the transport is in the northward (+) and southward (−) direction, respectively. "Total" is the sum of the two. The times of the sections are given in Table 4. The values for POM are averaged over two tidal cycles (~25 h) and centered on midday on the date given in Table 4. The values for SINMOD are based upon instantaneous sections at the following dates and times: Section I: 14 March 1988 00:00, Section II: 16 March 1988 12:00, Section III: 20 March 1988 12:00, Section IV: 21 March 1988 04:00, and Section IV′: 25 March 1988 20:00.

in Fig. 1b, using the velocity component normal to the section. The depth range was limited to the upper 250 m.

In the case of the observations, the ADCP velocities from 10, 14, 18, 22, 26, 30, 34, 38, 46, 54, 62, 70, 86, 102, 118, 134, 166, 198, 222, and 242 m were used, dependent on the water depth. For water depths less than 250 m, the deepest observation used was that nearest to 80% of the water depth. Below this depth the ADCP is known to return data of questionable quality, and the ADCP data below this depth were, therefore, replaced by a linear decrease to zero velocity at the bottom. The ADCP configuration and preprocessing are described in JH. For the transport calculations, an additional spatial low-pass filter with a 5 km cut-off was applied.

Vertical sections from POM were supplied as averages over the time span of the ship's track; the results were interpolated to 50 points in the horizontal, regardless of the length of the section. Vertical sections from SINMOD were supplied at a series of times (every 4 hours) covering the ship's track and at the approximate model grid spacing (4 km); the values in Table 5 refer to the specifically chosen instantaneous sections. For both models, the supplied vertical sections of normal velocity were first interpolated to a denser grid as a step in contour plotting (see Subsection 5.3 below); the volume transport to 250 m was then calculated from the gridded values.

A simple regression analysis of the *total* transport gives

$$\begin{aligned} &\text{POM} = 0.63 \cdot \text{DATA} + 0.71, \\ &\quad r^2 = 0.27, \\ &\text{SINMOD} = 0.50 \cdot \text{DATA} + 0.63, \\ &\quad r^2 = 0.24, \\ &\text{SINMOD} = 0.76 \cdot \text{POM} + 0.10, \\ &\quad r^2 = 0.82. \end{aligned} \tag{5.1}$$

In a statistical sense, the model-observation comparison is not good. Squared correlation coefficients (r^2) less than 0.3 indicate only a weak correlation. However, a regression analysis of the northward (positive) component alone shows that the northward transport is much better reproduced by the two models, viz.,

$$\begin{aligned} &\text{POM} = 1.18 \cdot \text{DATA} - 0.08, \\ &\quad r^2 = 0.78, \\ &\text{SINMOD} = 0.92 \cdot \text{DATA} + 0.01, \\ &\quad r^2 = 0.85, \\ &\text{SINMOD} = 0.71 \cdot \text{POM} + 0.15, \\ &\quad r^2 = 0.91. \end{aligned} \tag{5.2}$$

An examination of the distribution of velocity in the vertical sections (see Subsection 5.3 below) indicates that much of the discrepancy is found in the deeper part of the sections (below 100 m). Also, the locations of the NAC and its associated meanders play a role.

It should also be noted that the transport estimates of the two models are much more in line with each other ($r^2 = 0.82$ and 0.91) than with the data. This indicates either that there are important physical processes which are left out of the models, or that those processes included are not known well enough to be given a proper parameterization. Further, since the two models reproduce the northward flow much better than the total transport, the northward flux may be a manifestation mainly of the specified large scale fluxes on the coarse mesh grid. However, if true, this implies that the northward flow in the Halten Bank area is sensitive to the specification of these large scale fluxes, and by implication to the nesting technique.

5.2. *Horizontal distributions*

For the observations, use is made of the objective analysis maps of temperature, salinity and velocity found in JH. These maps are to be viewed as a "smart" interpolation, where also the temporal scale is taken into account. No further processing of these maps has been performed here. The horizontal fields supplied from POM were constructed from model results averaged over two tidal cycles ($\sim$25 h), which were supplied at 24-h intervals, i.e., one field per day for each area. From SINMOD, instantaneous horizontal fields were supplied at a series of times (every 6 h) encompassing the time span of the ship surveys, and as a superset of the mapping area at the model grid spacing (4 km).

To facilitate the comparison, the salinity, temperature and velocity fields from the observations and both models were plotted in the same map projection and with the same contour intervals. A selection of these maps at the 25 m level is included here in Figs. 2–4. A more complete set is found in Hackett and Røed (1992).

In making a comparison of these fields, the disparity in their temporal sampling must be kept in mind. The two model fields have different sampling (diurnal averages and instantaneous), but they are consistent for each of the three areas. In the objectively analyzed observed fields, on the other hand, a constant e-folding time scale (2.5 days) was used, but the temporal information is affected by time span of the data collection. For example, in the case of a long survey (several days), there may be significant changes in the velocity field, e.g., movement of an eddy structure through the area. The objective analysis then tends to smooth the structure of the synoptic velocity field. For this reason, maps showing the instantaneous velocities along the ship's track are included in Fig. 5. (These also serve to show the data coverage, i.e., they indicate where the objective analysis is interpolating and extrapolating.) Thus, the objective map of area A (Fig. 2a) which is quasi-synoptic and has no intersecting tracks, agrees very well with the instantaneous observations (Fig. 5a), while the objective maps of areas B and C (Figs. 3a, 4a), which span 2–3 days and have many intersecting tracks, show some significant deviations from the instantaneous observations (Figs. 5b, 5c). The corresponding objective maps of temperature and salinity (Figs. 2d, 2g, 3d, 3g, 4d, 4g) are probably affected in the same manner.

A comparison of the velocity fields from the observations and the models (Figs. 2a, 2b, 2c, 3a, 3b, 3c, 4a, 4b, 4c) leads to the following general conclusions: (a) both models are able to produce a northward flow at the coast and at the shelf break; (b) the POM velocities are generally of the right order of magnitude, while the SINMOD values are too small; (c) there is more of an "eddy zoo" in the POM fields than in the SINMOD fields, i.e., POM is more free to generate eddies and meanders while SINMOD is more restrictive; (d) the eddy and meander structures generated by the models are not located "correctly;" (e) in the Halten Bank area (area C, Fig. 4a), both models do fairly well in reproducing the coastal jet and the weak flow near the bank.

There is also an occasion where the models appear to be successful in reproducing eddies at about the right place. In area A (Fig. 2), the observations show a cyclonic eddy in the central part of the area and an anticyclonic eddy in the southwest corner (Figs. 2a, 2d, 2g). POM produces a cyclonic eddy somewhat further to the northeast (Figs. 2b, 2e, 2h), while SINMOD has an anticyclonic eddy nearer the coast (Figs. 2c, 2f, 2i). Neither model has both structures clearly defined. Satellite IR images (see Fig. 1a of Haugan et al., 1991) show that the observed structures are associated with cross slope exchanges; the cyclonic eddy is a core of Atlantic water which has intruded onto the shelf, while the anticyclonic eddy is connected with a bulge in the shelf break front. While the models have elements of these cross-slope features, they do not reproduce the observed intensity of the

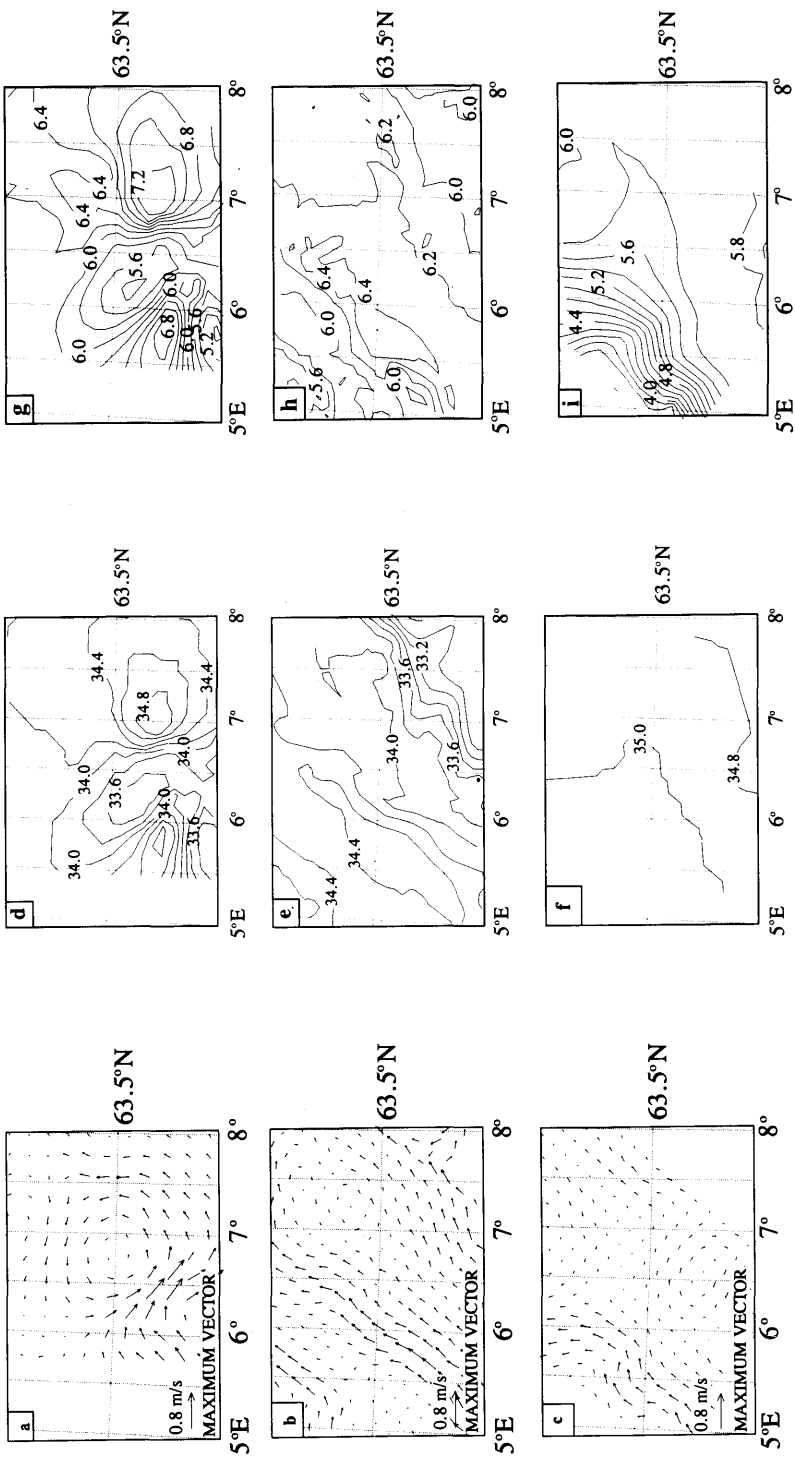

Fig. 2. Horizontal distributions of velocity (a, b, c), salinity (d, e, f), and temperature (g, h, i) at 25 m depth for area A (cf. Fig. 1b and Table 3). In each sequence of three the first corresponds to the objectively analyzed NORCSEX'88 data, the second to the similar POM model product, and the third to the similar SINMOD model product. Currents (a, b, c) are depicted as arrows in which the length of the arrow corresponds to the speed (see scale at bottom left), and the arrowhead points in the direction of the current. Solid lines in (d, e, f) show contours of salinity in practical salinity units (psu) with a contour interval of 0.2 psu. Solid lines in (g, h, i) show contours of temperature in °C with a contour interval of 0.2°C.

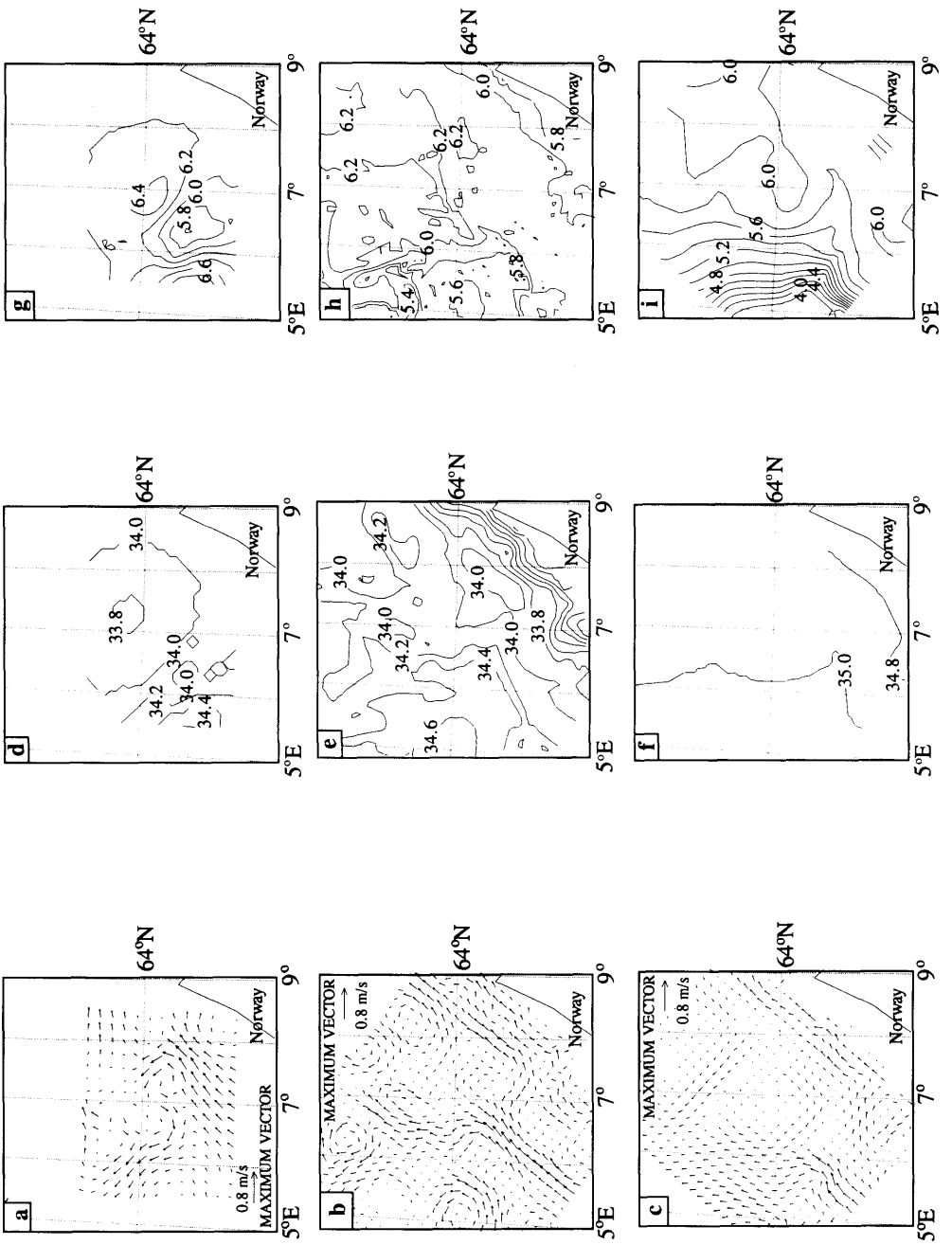

Fig. 3. As Fig. 2, but for area B.

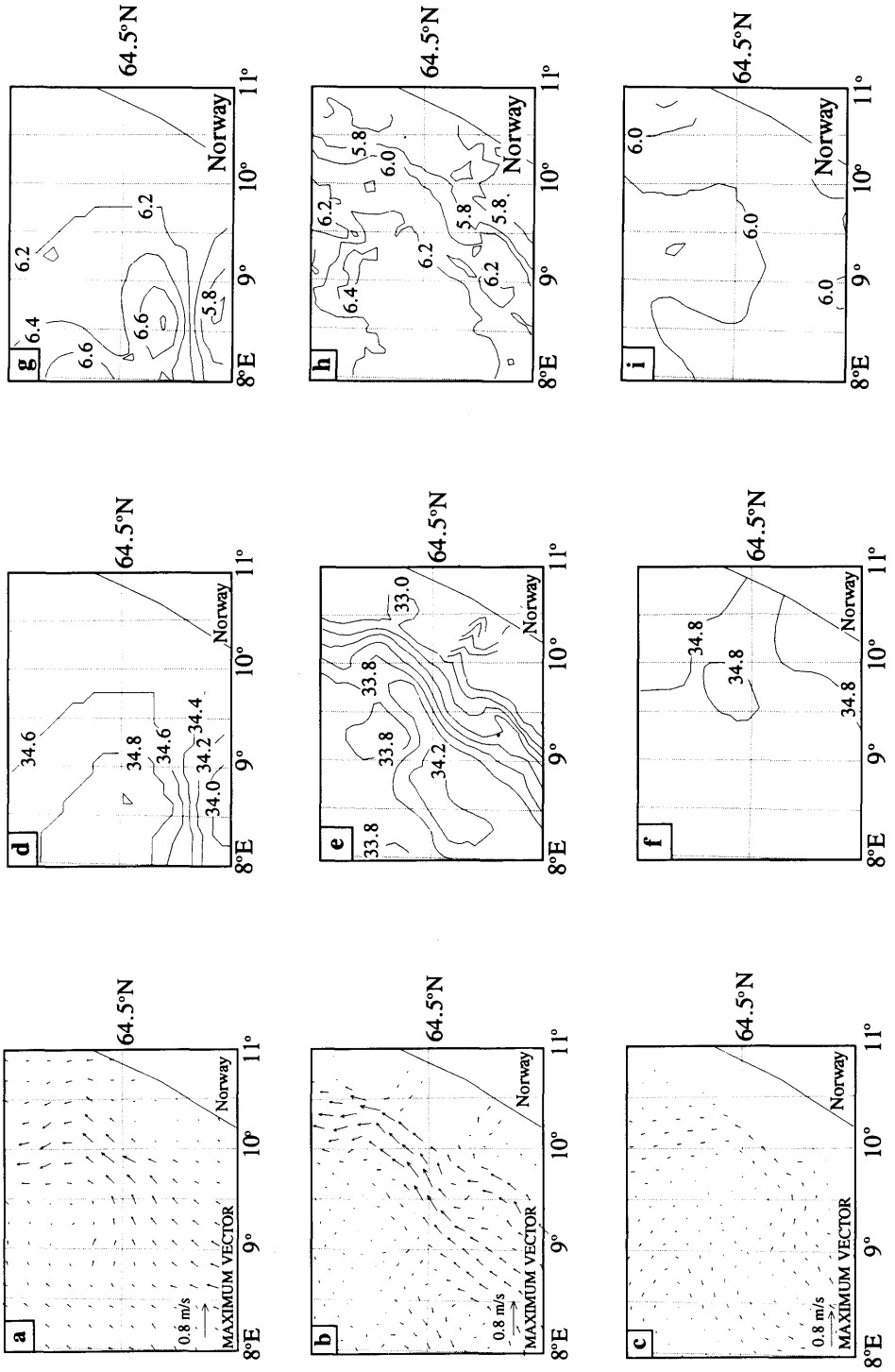

Fig. 4. As Fig. 2, but for area C.

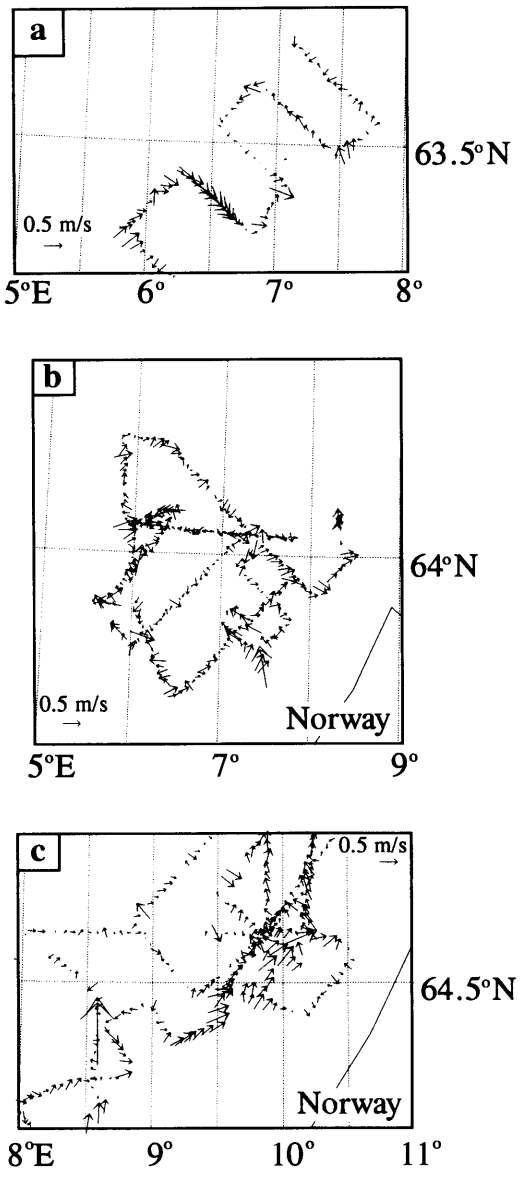

Fig. 5. Instantaneous ADCP velocity along the ship's track for the horizontal mapping areas A (a), B (b) and C (c). See Fig. 1b and Table 3.

exchange, in the sense of strong flows crossing the slope at an acute angle.

A comparison of the currents at several levels (other levels not shown here) shows that the vertical shear in the models is less than that observed, especially for the SINMOD model. This will be addressed in detail in the following section (vertical distributions).

Extending the comparison to include the instantaneous ADCP velocities (Fig. 5) indicates that the POM results agree better with the objectively analyzed fields, while the SINMOD results fare better when compared with the instantaneous currents. This suggests that the objective analysis tends to apply the same kind of smoothing to the data as the averaging used in the POM fields.

In the salinity and temperature fields, the models appear to differ considerably from the observations. This is particularly true for SINMOD, the reasons for which will become apparent in the following section (vertical distributions). POM, on the other hand, actually has a number of features which are qualitatively reproduced. Recalling that attention must be restricted to the areas in which there is actual data coverage, there are instances of maxima and minima in POM which agree generally with the observed fields. For example, in area B the model reproduces quite well the salinity maximum in the southwest and the minimum to the northeast (Figs. 3d, 3e). There are also positive points in POM's salinity field in area C (Figs. 4d, 4e). However, in area A, POM has no indication of the off-shore salinity minimum seen in the observations (Figs. 2d, 2e). Furthermore, POM seems to be less consistent than the observations in keeping temperature and salinity positively correlated.

5.3. Vertical distributions

The data and the model results used here are the same as those described in Subsection 5.1. First, consider section II, which extends from the continental shelf break to mid-shelf (cf. Fig. 1b). The observed current structure (Fig. 6a) shows cores of northward and southward flow near the shelf break, and generally southward flow over the shelf. Both models present the same qualitative picture: northward flow at the shelf break and at mid-shelf, with a weak southward flow between. In other words, neither model reproduces the countercurrents near the shelf break, and both produce a northward flow at mid-shelf, which is barely indicated in the observations. POM appears to reproduce the velocity magnitude and vertical shear somewhat better than SINMOD, whose velocity field is much smoother and has weaker gradients. The large discrepancies found in the

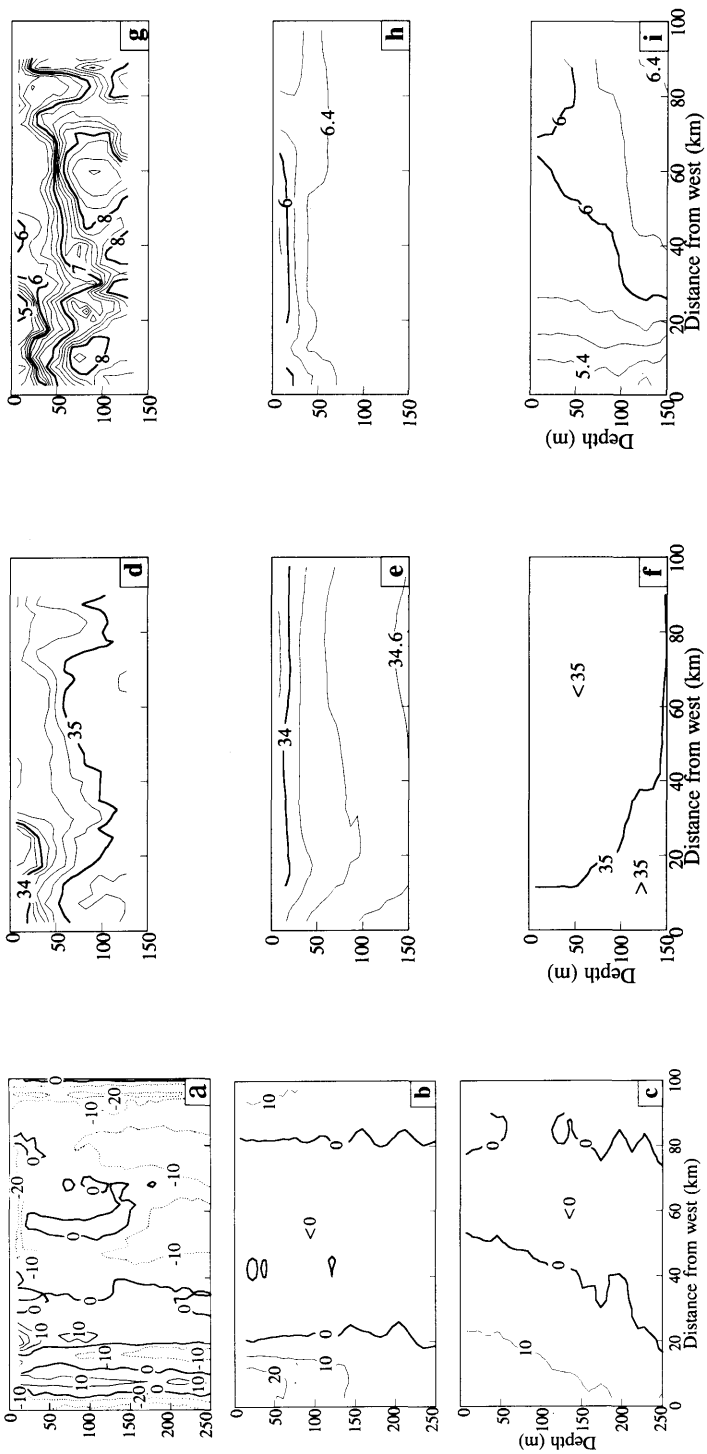

Fig. 6. Vertical sections of normal velocity (a, b, c), salinity (d, e, f) and temperature (g, h, i) for cross-section II (cf. Table 4 and Fig. 1b). In (a, b, c) the contour interval is 10 cm/s and positive velocities are into the page. In (d, e, f) the contour interval is 0.2 psu. In (g, h, i) the contour interval is 0.2°C. The upper (a, d, g), middle (b, e, h) and lower (c, f, i) panels contain the NORCSEX'88 ship observations, the POM model results and the SINMOD model results, respectively. The vertical and horizontal scales are indicated on the lower panels.

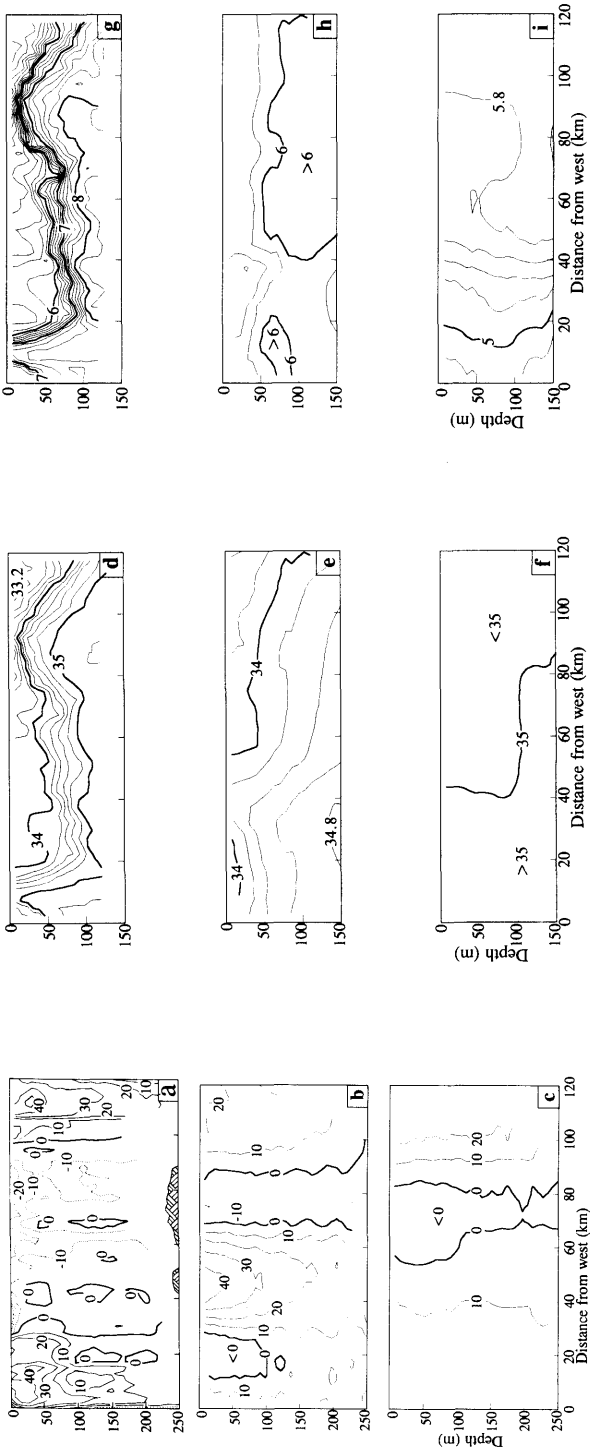

Fig. 7. As Fig. 6, but for cross-section III (cf. Table 4 and Fig. 1b).

Table 6. *Ranges of normal velocity, temperature and salinity in vertical section II*

Variable	Observations	POM	SINMOD
Normal velocity	−0.20–+0.30	−0.05–+0.25	−0.05–+0.15
Temperature	5.00°–8.50°	5.50°–6.50°	5.25°–6.25°
Salinity	33.5–35.1	33.7–34.7	34.9–35.05

All values estimated from contour plots, generally the smallest and largest contour lines drawn.

total volume transport (Table 5) are thus due to underestimation of the southward flow, especially at the ends of the section.

The salinity and temperature fields in Fig. 6 show more dramatic differences between the observations and models, and between the models. First, there is much more vertical and horizontal structure in the observations than in either model. Two important observational features are the lenses of coastal water (cold and brackish) near the shelf break—a remarkable feature in itself—and the deeper cores of Atlantic water (warm and saline), neither of which are reproduced in the models. Furthermore, the smoothness and weak gradients of SINMOD's fields is striking. Second, the range of values, which is summarized in Table 6, varies widely. In terms of the T–S (temperature–salinity) characterization of water masses, POM contains typical coastal water, but lacks the Atlantic water ($S > 35$). The water masses shown by SINMOD are impossible to identify in terms of the observed T–S properties.

Next, consider section III, which extends across the southern part of the shelf from the shelf break to the coast (cf. Fig. 1b). The observed current field (Fig. 7a) shows strong northward cores at the ends of the section, i.e., at the slope (NAC) and at the coast (NCC), with weaker southward flow on the shelf between. Both models succeed in reproducing all three of these features (cf. Figs. 7b, c). Again, SINMOD's velocities and gradients are much weaker than those observed. POM produces an apparently additional strong core of northward flow at mid-shelf. Examination of a time sequence of the horizontal distribution of currents (not shown) indicates that this velocity core is a filament of the NAC intruding onto the shelf, and the southward flows on either side are due to cyclonic and anti-cyclonic eddies forming on the flanks of the filament. Thus, POM errs in the placement of the NAC by allowing it to move onto the shelf. Accepting this, POM's velocities agree quite well with the observations for the slope current, but are still weaker than observed for the NCC. Both models show a deeper penetration of the northward flowing currents, i.e., weaker vertical gradients.

The salinity and temperature fields in Fig. 7 show many of the same characteristics as described for section II, and the same comments apply (cf. Table 7). In the case of POM, the horizontal distribution does bear a better resemblance to the observations, assuming that the slope current is "moved back" to the slope.

Most of the features pointed out here are also present in the remaining sections I, IV and IV′, which will not be discussed here. However, in the evaluation below, the analyses of all five vertical sections are taken into account.

5.4. *Evaluation*

Both models reproduce the general large scale circulation pattern of the mid-Norwegian shelf well. The two major currents, i.e., the NCC at

Table 7. *Ranges of normal velocity, temperature and salinity in vertical section III*

Variable	Observations	POM	SINMOD
Normal velocity	−0.30–+0.50	−0.10–+0.45	−0.05–+0.25
Temperature	4.75°–8.25°	5.50°–6.00°	4.75°–5.75°
Salinity	33.2–35.2	32.7–34.9	34.95–35.00

All values estimated from contour plots, generally the smallest and largest contour lines drawn.

Tellus A 46/2-3

the coast and the NAC at the shelf break, are found at about the proper places. The circulation on the shelf is variable, with clear effects of the topographic features (banks, troughs). On the other hand, a more detailed look shows that the two currents are broader, less vertically sheared and have smaller maximum velocities than the observations. This is particularly the case for the SINMOD results.

POM appears to be more amenable to producing meanders of the major currents and eddies. This indicates that the effect of eddy diffusivity and eddy viscosity is smaller than in the SINMOD model. For example, filaments of the NAC are seen to penetrate onto the shelf. Although this is not found in the observations at the same time and location as in the POM simulation, it is a well known feature in the area.

The SINMOD model did well in reproducing at least one example of an eddy forming in the coastal current. The POM model results do not show as good an agreement with observation on this occasion, but the averaging used makes an evaluation difficult.

The special dynamics of the shelf break region are evident in the observations, i.e., cross-shelf interchanges, narrow jets, etc., but the models are unable to reproduce them well. POM apparently is able to produce the right kind of motion, i.e., intrusions of Atlantic water onto the shelf, with accompanying eddy formation, but not at the times such structures were observed and not with the intensity observed.

The NORCSEX'88 observations are a good example of the classical observational picture of the hydrography of Norwegian shelf waters in the winter and spring (cf. Section 2). The models, on the other hand, are not. Neither model produces the observed ranges of salinity and temperature, although POM is far closer. The SINMOD results indicate, in fact, a T–S relationship which is opposite to that observed, i.e., temperature and salinity are negatively correlated. In addition, SINMOD's range of salinities is so (unrealistically) small that the density is determined more by temperature. In the case of POM, the ranges of temperature and salinity values are about 50–80% of the observed range; it is the Atlantic water mass (warm, saline) which is missing, at least within the depth range of the observations.

Both models produce smoother hydrographic fields than the observations, in the sense that the gradients and the ranges of values are smaller. This is particularly true for the SINMOD vertical fields, which moreover have gradients in the wrong direction due to an unrealistic T–S relationship. The smoother than observed fields from POM may be due to temporal averaging, although they display much more small scale structure and larger gradients than the SINMOD counterparts.

6. Summary and discussion

The results from a simulation of currents, temperature and salinity in March, 1988 for the Halten Bank area (an area located on the mid-Norwegian shelf) utilizing two fully three-dimensional, primitive equation, baroclinic level models (arbitrarily named POM and SINMOD) are considered. The results are compared against each other and with observations collected during the 1988 Norwegian Continental Shelf Experiment (NORCSEX'88). The comparison has been carried out on a hierarchical basis, starting with the most integral quantities, namely the transport through vertical sections and mean horizontal circulation, and then considering the details of selected horizontal and vertical distributions.

The evaluation of the model results and the observations indicates that the models are able to generate many features of the observed flow, but are unable to reproduce the detailed current observations, for instance the current observations at a point, to any required precision. The models' successes are attributable to inclusion of the important mechanisms for generating and maintaining currents in the Halten Bank area: the barotropic mode, baroclinic modes and nonlinearity. Their shortcomings stem from two main sources: the parameterization of subgrid turbulent mixing and horizontal resolution.

Consider, first, the turbulent parameterizations. In comparing the two models, the main point of *similarity* is that they both belong to the class of level models. As such, they both parameterize oceanic mixing by diffusion and eddy viscosity in the horizontal and vertical directions rather than along and across surfaces of equal density (isopycnals). There is evidence that mixing by mesoscale eddies in the ocean takes place predominantly along isopycnals, and that, consequently, diapyc-

nal mixing is rather small. By parameterizing subgrid turbulence with constant and rather large horizontal mixing, level models introduce a fictitious horizontal buoyancy flux, or equivalently, a large diapycnal mixing in areas of sloping isopycnals (Huang and Bryan, 1987; Drijfhuot, 1992). The main *difference* between the two models lies in how they implement the horizontal and vertical mixing processes. By using a turbulence closure scheme in the vertical and the Smagorinsky scheme in the horizontal, the POM model is the more sophisticated. Since the results indicate that the POM model fares better than the SINMOD model when compared with the observations, it may be concluded that the parameterizations employed are based on sound physical understanding. This is in accord with the GESAMP (1991) report, which states that the use of increasingly more sophisticated and complex formulations of these processes does not in itself reduce the uncertainty in the final model results, *unless* the physics of those processes is well understood.

The effect of the different mixing parameterizations is clearly shown in comparing the total transport through vertical sections and the detailed structure in those sections. Although the two models differ widely in their detailed velocity structures, the volume transports they produce are quite similar (cf. Table 5). This indicates that the transport is somewhat insensitive to the actual parameterizations chosen for the turbulent vertical eddy viscosity and diffusivity, while the current structure is highly sensitive to those parameterizations.

In comparison with the data, both models have trouble reproducing the strong vertical and horizontal velocity gradients observed, with POM performing better than SINMOD. Even the POM model, which has here been found to use superior parameterizations of the subgrid turbulence, generates too weak gradients. The models' shortcomings are most clearly revealed in the salinity and temperature fields, where both the ranges and gradients are underestimated (for SINMOD, greatly so). To be fair, some of the models' problems on this count may be attributable to the use of the Levitus hydrography, which is climatic and therefore very smooth, for initialization.

Next, consider the horizontal resolution. This is probably the foremost limiting factor for detailed modelling of current structures, i.e., eddies, especially at high latitudes. In general, the eddy scale (or mesoscale) is dictated by the internal Rossby radius of deformation, which decreases dramatically with latitude. Based on NORCSEX'88 data, the radius of deformation in the Halten Bank area is 5–10 km. The fine mesh grid size of the models, on the other hand, is 4 km (giving a Nyquist wave length of 8 km), which only barely, if at all, resolves this important length scale. (Note that this grid size was stipulated from the outset and was not left to the discretion of the modelers.) As noted by Treguier (1992), Böning and Budich (1992), and also by Semtner and Chervin (1992), it is imperative to resolve the radius of deformation in order to obtain a correct representation of the eddy field even in a statistical sense. For the Halten Bank area, a model grid size of about 2 km would seem appropriate. With models of the size and complexity used here, a major (perhaps *the* major) obstacle to their use in providing detailed information on currents in the area is, therefore, limited computer resources.

The effect of insufficient resolution is evident in the discrepancies between the detailed current structures in the models and the observations. For one thing, eddy structures on the scale of 5–10 km have indeed been found to be ubiquitous in the area, with a major impact on the currents (Haugan et al., 1991). Models with the resolution used here will have difficulty in reproducing these features, and rather will place the eddy energy on somewhat larger length scales. Another problem is the models' difficulties in placing the NAC correctly, which points to the general problem of cross-slope interaction processes. It is here that the models give the largest discrepancies, and it is believed that, again, this is largely due to their inability to resolve those processes. It should be noted, however, that the rather low resolution of the coarse mesh grid (20 km) may also play an important role for the models' behavior in the slope region.

A related point is the fact that both models are better able to reproduce the northward volume transport than the total transport. This may indicate that the northward flux is mainly a barotropic response and is a manifestation primarily of the specified large scale fluxes in the coarse mesh grid. If true, this implies that the northward flow in

the Halten Bank area is sensitive to the specification of these large scale fluxes.

In conclusion, the evaluation of the model results and the subsequent validation clearly indicates that neither model is able to reproduce the detailed current observations, for instance the current observations at a point, to any required precision. This conclusion is based on the two models' inability to *quantitatively* reproduce the detailed vertical and horizontal structures seen in the observations. This is mainly attributed to the too course resolution of the models, i.e., their inherent inability to reproduce the eddy field because of the 4 km grid. On the other hand, POM shows the promise of being able to reproduce the observed features in a statistical sense, i.e., producing the right kinds of structures with a realistic range of values. There is therefore reason to believe that, provided that the resolution is increased (finer mesh size) and provided that the horizontal eddy viscosity is kept to a minimum, the POM model may by used to predict the currents in the Halten Bank area in a statistical sense, i.e., to predict the mean current and its variability. This conclusion is based on the model's ability to *qualitatively* reproduce many of the vertical and horizontal structures seen in the observations, particularly the temperature and salinity distributions and the T–S relationship.

Finally, on the basis of the conclusions from this study, there is reason to believe that a better validation could be achieved by an increased horizontal resolution. Due to the computational burden, this is costly to achieve with the two-level models presented here. However, this could be achieved by sacrificing some vertical resolution in order to gain better horizontal resolution, for instance by employing a less complex model, e.g., an isopycnal model along the lines suggested by Bleck et al. (1992) or the even simpler layered model suggested by McCreary et al. (1991). The observations indicate that the motion is trapped into the barotropic (external) and only the first few baroclinic (internal) modes. Such a system indeed favors a layered model with two or three active layers, in which exchange between the barotropic and baroclinic modes is through the non-linear advection terms. It is, however, important that even the simplest model allow for advection of temperature and salinity in the upper layer(s), and that entrainment of lower layer water masses be included to allow for (controlled) mixing across isopycnals.

7. Acknowledgments

The simulation results from the two models used in the present study were most kindly supplied to us by Prof. L.-Y. Oey of Stevens Institute of Technology, New Jersey (POM model) and Dr. D. Slagstad of SINTEF, Trondheim, Norway (SINMOD model) as part of the Metocean Modeling Project, MOMOP. MOMOP is funded by the OKN Group, a consortium consisting of Den norske stats oljeselskap (STATOIL) A/S, Norsk Hydro A.S., Saga Petroleum a.s., Phillips Petroleum Co. Norway, A/S Norske Shell, Mobil Expl. Norway Inc., Esso Norge A.S., Elf Aquitaine Norge A/S, BP Petroleum Dev. Norway Ltd, Total Marine Norsk A/S, and Conoco Norway Inc. The support of the OKN Group, which made this investigation possible, is gratefully acknowledged. The NORCSEX'88 data was supplied to us by J. A. Johannessen and P. M. Haugan at the Nansen Center main office (Bergen). We would also like to thank them, L.-Y. Oey and D. Slagstad for many helpful comments during various stages of this research.

REFERENCES

Bleck, R., Rooth, C., Hu, D. and Smith, L. T. 1992. Salinity-driven thermocline transients in a wind- and thermohaline-forced isopycnic coordinate model of the North Atlantic. *J. Phys. Oceanogr.* **22**, 1486–1505.

Blumberg, A. F. and Mellor, G. L. 1987. A Description of a Three-Dimensional Coastal Ocean Circulation Model. In: *Three-dimensional coastal ocean models*, ed. Norman S. Heaps, Coastal Estuarine Sci. Ser., Vol. 4, AGU, Washington, DC, pp. 1–16.

Böning, C. W. and Budich, R. G. 1992. Eddy dynamics in a primitive equation model: Sensitivity to horizontal resolution and friction. *J. Phys. Oceanogr.* **22**, 361–381.

Chassignet, E. P. 1992. Rings in numerical models of ocean general circulation: a statistical study. *J. Geophys. Res.* **97** (C6), 9479–9492.

Drijfthut, S. S. 1992. Ring genesis and the related heat transport. Part II: A model comparison. *J. Phys. Oceanogr.* **22**, 268–285.

Eide, L. I. 1979. Evidence of a topographically trapped vortex on the Norwegian Continental Shelf. *Deep Sea Res.* **26** (6A), 601–621.

Engedahl, H. and Martinsen, E. A. 1988. Documentation of the two-dimensional ocean model at DNMI. *Tech. Rep. no. 67*, Det norske meteorologiske institutt, Oslo, Norway.

Gammelsrød, T. and Hackett, B. 1981. The circulation of the Skagerrak determined by inverse methods. In: *The Norwegian coastal current*, vol. II, eds. R. Sætre and M. Mork, Geilo, Norway, 1980, 311–330.

GESAMP (IMO/FAO/UNESCO/WMO/WHO/IAEA/UN/UNEP Joint Group of Experts on the Scientific Aspects of Marine Pollution), 1991: *Coastal Modelling*, GESAMP Reports and Studies No. 43, 192 pp.

Gjevik, B. and Straume, T. 1989. Model simulation of the M_2 and K_1 tide in the Nordic Seas and the Arctic Ocean. *Tellus* **41A**, 73–96.

Hackett, B. and Røed, L. P. 1992. MOMOP Phase 2. Evaluation of models and influence of data assimilation (I). Evaluation of two baroclinic ocean models for the Halten Bank region. *Tech. Rep. no. 49*, Nansen Environmental and Remote Sensing Center, Lysaker, Norway.

Haugan, P. M., Evensen, G., Johannessen, J. A., Johannessen, O. M. and Petterson, L. H. 1991. Modeled and observed mesoscale circulation and wave-current refractions during the 1988 Norwegian Continental Shelf Experiment. *J. Geophys. Res.* **96** (C6), 10,487–10,506.

Hellerman, S. and Rosenstein, M. 1983. Normal Monthly Wind Stress over the World Ocean with Error Estimates. *J. Phys. Oceanogr.* **13**, 1093–1104.

Huang, R. X. and Bryan, K. 1987. A multilayer model of the thermohaline and wind-driven ocean circulation. *J. Phys. Oceanogr.* **17**, 1090–1924.

Johannessen, J. A. 1991. The Norwegian continental shelf experiment prelaunch ERS 1 investigation. *J. Geophys. Res.* **96** (C6), 10,409–10,410.

Johannessen, J. A. and Haugan, P. M. 1991. A MOMOP Study: Processing and Presentation of NORCSEX'88 Oceanographic Data. *Technical Report no. 37*, Nansen Environmental and Remote Sensing Center, Bergen, Norway.

Levitus, S. 1982. Climatological atlas of the world ocean. *NOAA Prof. pap. 13*, US Dep. of Commerce, NOAA, Rockville, Maryland.

Martinsen, E. A., Røed, L. P. and Gjevik, B. 1979. A numerical model for long barotropic waves and storm surges along the western coast of Norway. *J. Phys. Oceanogr.* **9**, 1126–1138.

McCartney, M. S. and Talley, L. D. 1984. Warm-to-cold water conversion in the northern North Atlantic Ocean. *J. Phys. Oceanogr.* **14**, 922–935.

McCreary, J. P., Fukamachi, Y. and Kundu, P. K. 1991. A numerical investigation of jets and eddies near eastern ocean boundaries, *J. Geophys. Res.* **96** (C2), 2515–2534.

Mellor, G. L. and Yamada, T. 1982. Development of a turbulence closure model for geophysical fluid problems. *Rev. Geophys. Space Phys.* **20**, 851–875.

Oey, L.-Y. and Chen, P. 1992a. A Nested-grid ocean model: With application to the simulation of meanders and eddies in the Norwegian Coastal Current. *J. Geophys. Res.* **97** (C12), 20,063–20,086.

Oey, L.-Y. and Chen, P. 1992b. A model simulation of circulation in the Northeast Atlantic shelves and seas. *J. Geophys. Res.* **97** (C12), 20,087–20,115.

Røed, L. P., Hackett, B. and Skåtun, H. 1989. Metocean Modeling Project (MOMOP): Final Report. Results of the model intercomparison (abridged version). *Veritec Report no. 89-3312*, Veritas Offshore Technology and Services A/S, Høvik, Norway, 70 p.

Semtner, A. J. and Chervin, R. M. 1992. Ocean general circulation from a global eddy-resolving model. *J. Geophys. Res.* **97** (C4), 5493–5550.

Slagstad, D. and Støle-Hansen, K. 1991. MetOcean MOdeling Project Phase 2. Results from SINMOD-3D. *SINTEF Report STF48 F91005*, 57 pp.

Slagstad, D. 1987. A 4-Dimensional Physical Model of the Barents Sea. *SINTEF Report STF48 F87013*, 34 pp.

Smagorinsky, J. 1963. General circulation experiments with the primitive equations. I: The basic experiment. *Mon. Wea. Rev.* **91**, 99–164.

Stern, M. E. 1975. *Ocean circulation physics*, Int. Geoph. Ser., Vol. 19, Academic Press.

Thompson, J. D. and Schmitz, W. J. 1989. A limited-area model of the Gulf stream: Design, initial experiments, and model-data intercomparison. *J. Phys. Oceanogr.* **19**, 791–814.

Treguier, A. M. 1992. Kinetic energy analysis of an eddy-resolving, primitive equation model of the North Atlantic. *J. Geophys. Res.* **97** (C1), 687–701.